AGU PUBLICATIONS

Geophysical Research Letters

RESEARCH LETTER
10.1002/2014GL059561

Key Points:
- Twenty year resolved water isotope record documents Marine Isotope Stage 5 temperatures
- Long-term changes are associated with changes in high-frequency variability
- Enhanced variability detected when East Antarctic climate was warmer

Supporting Information:
- Readme
- Text S1
- Text S2
- Text S3
- Table S1
- Table S2
- Figure S1
- Figure S2
- Figure S3
- Figure S4
- Figure S5
- Figure S6
- Figure S7
- Figure S8

Correspondence to:
K. Pol,
katl@bas.ac.uk

Citation:
Pol, K., et al. (2014), Climate variability features of the last interglacial in the East Antarctic EPICA Dome C ice core, *Geophys. Res. Lett.*, *41*, 4004–4012, doi:10.1002/2014GL059561.

Received 14 FEB 2014
Accepted 26 APR 2014
Accepted article online 30 APR 2014
Published online 6 JUN 2014

Climate variability features of the last interglacial in the East Antarctic EPICA Dome C ice core

K. Pol[1,2], V. Masson-Delmotte[1], O. Cattani[1], M. Debret[3], S. Falourd[1], J. Jouzel[1], A. Landais[1], B. Minster[1], M. Mudelsee[4,5], M. Schulz[6], and B. Stenni[7]

[1]Laboratoire des Sciences du Climat et de l'Environnement, IPSL, UMR 8212 CEA CNRS UVSQ, Gif-Sur-Yvette Cedex, France, [2]British Antarctic Survey, Cambridge, UK, [3]Laboratoire De Morphodynamique Continentale et Côtière–UMR CNRS 6143, Université de Rouen, Mont Saint Aignan Cedex, France, [4]Alfred Wegener Institute for Polar and Marine Research, Climate Science Division, Bremerhaven, Germany, [5]Climate Risk Analysis, Bad Gandersheim, Germany, [6]MARUM–Center for Marine Environmental Sciences and Faculty of Geosciences, University of Bremen, Bremen, Germany, [7]Department of Mathematics and Geosciences, University of Trieste, Trieste, Italy

Abstract Whereas millennial to submillennial climate variability has been identified during the current interglacial period, past interglacial variability features remain poorly explored because of lacking data at sufficient temporal resolutions. Here we present new deuterium data from the EPICA Dome C ice core, documenting at decadal resolution temperature changes occurring over the East Antarctic plateau during the warmer-than-today last interglacial. Expanding previous evidence of instabilities during the last interglacial, multicentennial subevents are identified and labeled for the first time in a past interglacial context. A variance analysis further reveals two major climatic features. First, an increase in variability is detected prior to the glacial inception, as already observed at the end of Marine Isotopic Stage 11 in the same core. Second, the overall variance level is systematically higher during the last interglacial than during the current one, suggesting that a warmer East Antarctic climate may also be more variable.

1. Introduction

Among other long palaeoclimatic records, the EPICA Dome C (EDC) ice core (75°06'S, 123°2'E, see insert of Figure 1) has contributed in a major way to characterize glacial/interglacial climate variability over the last 800 thousand years (hereafter kyr), by providing multiproxy records of climate and atmospheric composition variations [*Jouzel et al.*, 2007; *Lambert et al.*, 2008; *Loulergue et al.*, 2008; *Luthi et al.*, 2008; *Siegenthaler et al.*, 2005; *Spahni et al.*, 2005; *Wolff et al.*, 2010]. Continuous 55 cm deuterium (δD) measurements (Figure 1) [*Jouzel et al.*, 2007] have in particular documented past EDC long-term temperature changes and evidenced recurrent millennial-scale variability of glacial periods, characterized by Antarctic Isotopic Maxima (AIM) events known as counterparts of rapid temperature changes in Greenland [*EPICA-community-members*, 2006; *Capron et al.*, 2010]. So far, Antarctic temperature variations during the last nine interglacial periods (cf. Figure 1)—occurring under global warm climatic conditions (e.g., surface temperatures, sea level, and sea ice extent) close to the modern ones—have shown differences in terms of shape, intensity, or duration [*Tzedakis et al.*, 2009]. While these features highlight the climate heterogeneity of interglacial periods at multimillennial scale, they do not bring evidence of higher-frequency climate variability at play during interglacial periods.

Well dated and highly resolved climate records of the current interglacial period have yet allowed one to document climatic variations expressed at millennial to submillennial scales, with regional specificities [e.g., *Masson et al.*, 2000; *Mayewski et al.*, 2004; *Wanner et al.*, 2008, 2011]. Understanding the mechanisms at play in such variability is important with respect to future climate change and climate predictability [*Braconnot et al.*, 2012; *Deser et al.*, 2012]. However, the dating uncertainties and the limited temporal resolutions associated with natural archives restrain the documentation of such high-frequency variability during previous interglacials. Ice core records are for instance affected by the thinning of ice layers in the ice sheet, which progressively compresses the climatic information (Figure 1) and increases chronological uncertainties [*Kawamura et al.*, 2010]. Yet palaeoclimatic records resolved at subcentennial scale and covering Marine Isotope Stage 5 [e.g., *Bigler et al.*, 2010; *Galaasen et al.*, 2014] or MIS 11 [*Koutsodendris et al.*, 2011; *Pol et al.*, 2011] have recently emerged, providing strong evidence that previous interglacial periods also experienced significant climatic variations at millennial to submillennial scale. However, it is still unknown whether all interglacial periods present the same patterns of variability and whether a link between this high-frequency climate variability and mean climatic states can be established.

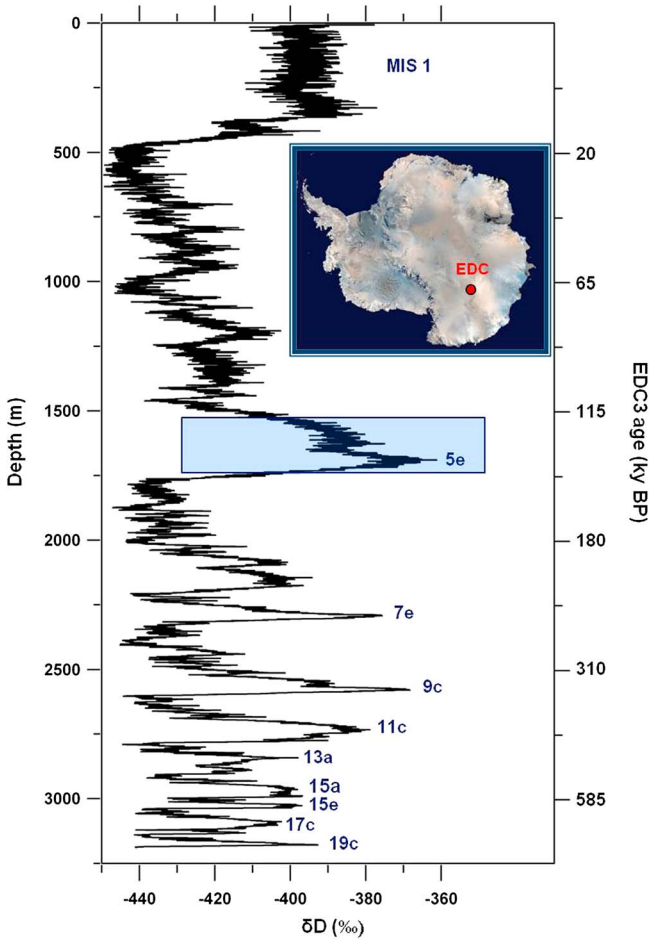

Figure 1. Vertical profile of the 55 cm EDC δD record (‰, bottom axis) along the ~3190 m of the core (left axis, see insert for the position of the EDC site over the East Antarctica plateau). Corresponding ages (right axis, kyr B.P.) are given using the EDC3 chronology [*Parrenin et al.*, 2007]. Interglacial periods are labeled with respect to the Spectral Mapping Project (SPECMAP) terminology [*Imbrie et al.*, 1984]. The blue-shaded area indicates the ice core section which has been analyzed at 11 cm resolution.

Here we address these questions for the last interglacial or MIS 5e (Figures 1 and 2, MIS 5 substages are nominated according to the marine SPECMAP terminology [*Imbrie et al.*, 1984], assuming that air surface and sea surface temperatures vary simultaneously in the subantarctic zone [*Govin et al.*, 2012]), by looking at different aspects of the climate variability: the occurrence of climatic subevents, detected changes in variance, and their potential connection with long-term trend changes. The last interglacial is of prime interest for three main reasons. First, due to its position in the EDC core, Antarctic temperature changes during MIS 5e can be described at the same 20 year temporal resolution as during MIS 1, using new δD measurements of 11 cm samples produced for the purpose of this study (see Text S2). Second, the existing EDC δD record exhibits an early isotopic optimum at the end of Termination II comparable to the MIS 1 early optimum (or AIM 0 [*Stenni et al.*, 2011]). Albeit occurring under different orbital configurations, both optima have been similarly hypothesized to reflect bipolar seesaw processes linked to reorganizations of the Atlantic Meridional Overturning Circulation (AMOC) [*Masson-Delmotte et al.*, 2010; *Stenni et al.*, 2011]. Third, MIS 5e is characterized by enriched Antarctic water stable isotope values reflecting a warmer than present regional climate (temperatures at least ~4.5°C above present day) [*Jouzel et al.*, 2007; *Sime et al.*, 2009] and a sea level high stand at least 5.5 m above today [*Dutton and Lambeck*, 2012; *Kopp et al.*, 2009], caused by reduced Greenland [*Dutton and Lambeck*, 2012; *NEEM-community-members*, 2013] and Antarctic ice sheets [*Bradley et al.*, 2012, 2013; *Holden et al.*, 2010; *O'Leary et al.*, 2013]. Therefore, it provides the most recent case study for understanding the climate/ice sheet interaction processes associated with warmer-than-today polar temperatures.

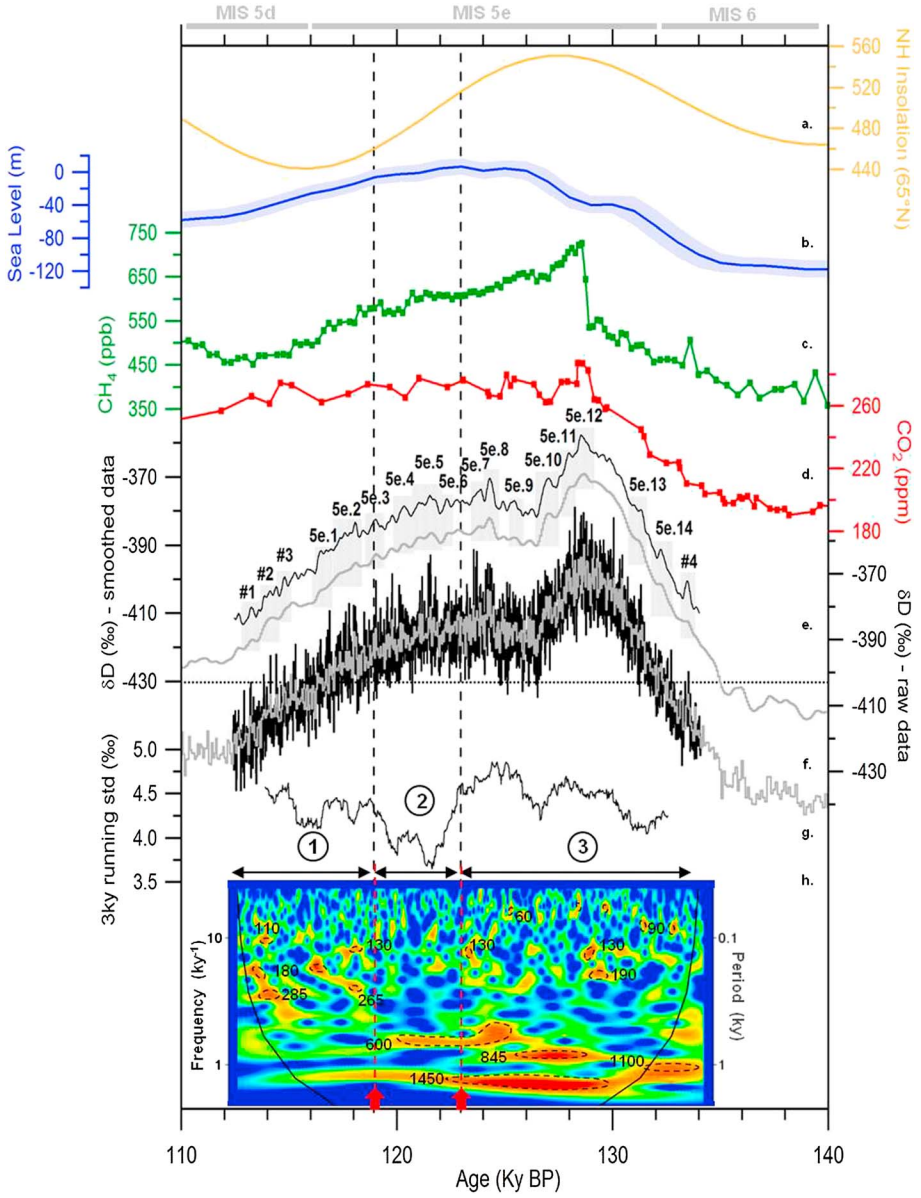

Figure 2. Climatic context and Antarctic temperature variability during the last interglacial. The studied interval extends from the glacial inception or MIS 5d (110 kyr B.P.) to the transition MIS 6/ MIS 5e or Termination II (140 kyr B.P., see delimited intervals on top). (a) Changes in summer insolation at 65°N (W m^{-2}, yellow). (b) Estimate of sea level changes according to *Kopp et al.* [2009] (in meter relative to present sea level, displayed in blue with the associated uncertainty in shaded blue). (c) EDC CH_4 concentrations (ppb, green) [*Loulergue et al.*, 2008; *Spahni et al.*, 2005]. (d) CO_2 concentrations from the EDC and Vostok ice cores (ppm, red) [*Luthi et al.*, 2008; *Siegenthaler et al.*, 2005]. Both GHG (for greenhouse gas) signals are plotted with respect to the EDC gas chronology [*Loulergue et al.*, 2007]. (e) Smooth δD signals (‰), derived from the 500 year binomial smoothing of the 20 year resampled (f) raw data (‰). Fifty-five centimeter samples in grey and 11 cm samples in black, shifted by a 10‰ offset on *y* axis; the noticeable events (see Figures 3c and 3h and section 2.1 in Text S2 for details) are highlighted by grey-shaded areas and labeled. (g) Running standard deviation over a 3 kyr window of the black δD signal of Figure 2f, resampled on a regular time step of 20 years and detrended (Text S1). Three different phases of variability have been identified (see section 2.2 of Text S2 and Figure S7 for the description of the method) and labeled 1, 2, and 3 (see black arrows); they are reported by black dashed lines over Figures 2a–2g. (h) Wavelet spectral analysis of the black δD signal of Figure 2f, resampled and detrended. The spectral power is displayed in function of time (kyr B.P.), frequency (left axis, 1/kyr), and corresponding periodicity (right axis, kyr). Black dashed contours delineate the significant periodicities, as the black line delineates the cone of influence (see Text S2). Red arrows and red dashed lines define the three different areas of variability identified in Figure 2f.

2. Data and Methods

Using the −403‰ δD threshold in the EDC core to define past interglacials [*EPICA-community-members*, 2004], the warm Antarctic phase of MIS 5e is found between depths of ~1531 m and ~1742 m in the EDC core, corresponding to a time interval ranging from ~116.3 ± 1.5 kyr to ~132.3 ± 6 kyr before present (hereafter B.P, see the dashed line on Figure 2f) according to the EDC3 chronology [*Parrenin et al*., 2007] (see section 1.2 of Text S2). We have here produced 2415 new δD measurements (11 cm length samples: see section 1.3 of Text S2) along a widened interval from ~1490 m (~112.4 kyr B.P.) to ~1756 m (~134 kyr B.P.) (blue area of Figure 1), in order to also encompass the penultimate termination (Termination II) and the onset of the glacial inception following the interglacial interval. Depending on the location in the core and therefore on associated changes in accumulation and thinning function (Figure 1) [*Parrenin et al*., 2007], the time step of our new record (black, Figure 2f) varies from 6 to 14 years against 30 to 70 years for the initial one (grey) (section 1.1 of Text S2). This new record is compared to the initial low-resolution profile (from 55 cm samples) on Figure 2f (respectively black and grey curves); both signals are given with an identical analytical accuracy of ± 0.5‰ at 1σ (see section 1.2 of Text S2). Our new data highlight isotopic variations showing amplitudes of up to 14‰ (2.5 higher than the ones exhibited in the initial record).

As demonstrated by a signal-to-noise study conducted at Vostok [*Ekaykin et al*., 2002], central Antarctic ice cores cannot, however, archive climate variability on time scales below ~20 years, due to postdeposition effects (e.g., wind scouring or isotopic diffusion, see section 1.1 of Text S2). Antarctic climate variations over MIS 5e are thus thereafter examined after a 20 year resampling, as previously done for MIS 1 [*Masson et al*., 2000; *Pol et al*., 2011]. Investigated features of the MIS 5e variability (climatic subevents, changes in variance and links between long-term trends and high-frequency variability) are compared to those extracted from the existing MIS 1 EDC δD data. We, however, note that such variability analyses in ice cores can be limited by two major critical points. First, the isotopic diffusion occurring both in the firnication zone [*Neumann and Waddington*, 2004] and in solid ice [*Ramseier*, 1967] can smooth or erase the highest-frequency climatic information in ice core isotopic signals. Our diffusion calculations for the EDC core (see section 1.4 of Text S2 and Figure S3) over MIS 1 and 5e intervals have shown that only climatic variations shorter than 6 years were affected by diffusion, thus allowing us to rule out any diffusive biases in our variance analyses performed on 20 year resolved records. Second, spectral analyses have been demonstrated to be highly dependent on chronology uncertainties [*Pol et al*., 2011]. Age-scale tests have therefore been performed to assess the reliability of the EDC3 chronology over our extended MIS 5e interval (see sections 1.3 and 3.3 of Text S2 and Figure S2) and to demonstrate the robustness of our results against given uncertainties [*Parrenin et al*., 2007; *Bazin et al*., 2013].

3. Results and Discussion

3.1. Detection of Interglacial Multicentennial Climatic Subevents

The added value of increasing the resolution of the EDC δD record over MIS 5e is first evidenced when examining our two signals (Figure 2f) at multicentennial scale. *Wanner et al*. [2011] used a 500 year binomial filter to highlight climatic events taking place during the current interglacial period in a large variety of records. For comparison, we applied the same filter both on our new 20 year resampled signal and on the initial 70 year resampled one (see section 2 of Text S2; results obtained from a reduced by a factor of 2 length of smoothing are also illustrated in Text S2). The resulting curve from the 20 year record (black, Figure 2e) reveals 18 climatic excursions (hereafter called climatic subevents and labeled SE) that were hardly distinguishable in the initial profile (grey, Figure 2e). The detection of these subevents has been conducted with respect to the methodology described in section 2.1 in Text S2 and Figure S4 (see also Figures 3c and 3h). They are labeled over the whole MIS 5e interval and independently numbered for the discontinuous MIS 5d and 6 segments (see Figure 2e and the delineated periods on top). Their respective duration, shape, and intensity are summarized in Table S1. All of them exhibit isotopic amplitudes of at least 4 ± 1‰, which can be converted into minimal temperature changes of 0.6 ± 0.15°C using the present-day spatial slope of 6‰/°C [*Jouzel et al*., 2007]. However, simulations performed with one atmospheric model equipped with water stable isotopes have suggested that the use of this spatial slope may lead to an underestimation of past temperature changes for warmer-than-today conditions, by at least 30% [*Sime et al*., 2009].

With the exception of the long SE 5e.2 and 5e.12 events which stretch over 1 kyr, our subevents are recorded at a typical centennial time scale. Eighty-five percent of those subevents are characterized by δD amplitudes ranging from 4 to 8 ± 1‰; three of them, however, stand out by showing δD amplitudes exceeding 9‰ (or temperature changes larger than 1.5°C): SE 5e.14 during Termination II, and SE 5e.8 and 5e.10 following the early MIS 5e isotopic maximum. They have been detected using the detrended record (see section 2.1 in Text S1 and Figure 3h); but when mapped back onto the original signal (Figures 2e and 3g.), three types of events can be distinguished, mainly depending on the variations of the long-term trend (displayed in Figure 3f in red) on which they are superimposed (see section 3.1 in Text S2): (i) warming events (SE 5e.13 and 5e.14), (ii) cooling events (SE #1, #2, and #3, 5e.1, 5e.2, 5e.10, and 5e.11), and (iii) triangular shape events (SE 5e.3 to 5e.9 and 5e.12 and SE #4). We, however, note that SE #4—albeit occurring on top of the dominating warming trend of Termination II—shows a standing-out triangular shape. Subevent 5e.2 over the glacial inception is also noticeable because of a prominent warming at its beginning, which contrasts with the following cooling trend. SE 5e.1 and 5e.13—showing a plateau instead of an isotopic excursion, respectively, at their start or end—can also be pointed out as they evidence a pause in the course of either the glacial inception or Termination II. Hence, while the majority of subevents are just superimposed onto the associated dominating long-term trend, the previous exceptions stand as hiatus in the natural multimillennial course of Antarctic climate variability.

Over the 12 kyr interval from 130 to 118 kyr B.P., we report 11 events (SE 5e.2 to SE 5e.13), including two events with δD amplitudes exceeding 8‰ (Table S1). Applying the same methodology (Figure 3c) over the equivalent ongoing MIS 1 11.7 kyr interval only shows five comparable subevents, with none of them showing δD amplitudes exceeding 8‰ (Figure 3b, see Table S2 for a detailed characterization). Assuming that the main features of the Antarctic climate variability are reliably recorded in the EDC δD signal [*Masson-Delmotte et al*., 2011], MIS 1 and 5e subevents demonstrate the recurrence of submillennial variability during the two last interglacial periods in Antarctica and suggest a more variable climate over the East Antarctica plateau during the warmer last interglacial period than during the current one.

Detected interglacial subevents in the EDC δD record show amplitudes high enough to be expected to witness larger-scale changes. For reference, temperature changes during the smallest glacial AIM (#9 and #13) are estimated, respectively, at 0.5 and 0.6°C over the East Antarctic plateau according to *Stenni et al*. [2010]. However, in the absence of a Greenland ice core record covering MIS 5e which could be used as a reference to investigate possible counterparts of the present subevents in the Northern Hemisphere [*EPICA-community-members*, 2006; *NEEM-community-members*, 2013], it is not possible to conclude about the large-scale relevance of present Antarctic subevents during the last interglacial. Clues for submillennial-scale variability in MIS 5e Antarctic greenhouse gas (GHG) records do exist [*Loulergue et al*., 2008; *Luthi et al*., 2008; *Siegenthaler et al*., 2005; *Spahni et al*., 2005] (Figures 2c and 2d); but an objective matching between δD and GHG features is limited by the resolution of existing GHG records, the loss of centennial variations caused by firn gas diffusion [*Spahni et al*., 2003] and the uncertainties linked to ice and gas-age differences [*Bazin et al*., 2013]. Referring to available records from different archives showing compatible instabilities over the MIS 5e—for instance in Europe [*Allen and Huntley*, 2009; *Drysdale et al*., 2009; *Milner et al*., 2013; *Müller et al*., 2005], Mediterranean [*Martrat et al*., 2004; *Sprovieri et al*., 2006], or North Atlantic [*Bauch and Kandiano*, 2007; *Galaasen et al*., 2014; *Oppo et al*., 2006] basins—would appear even trickier in the absence of synchronized age scales. Concluding about the spatial representativeness of such interglacial subevents would thus require further investigations which are beyond the scope of the present paper.

3.2. Characterization of the Antarctic Climate Variability During the Last Interglacial Period

We now consider the full range of information contained in our detailed EDC δD record in order to investigate changes in Antarctic high-frequency climate variability. After removing the climatic long-term trend (shown in Figure 3f, red, for the 118–130 kyr B.P. interval, see section 2.2 in Text S2 for details) from our 20 year resampled signal, a 3 kyr running standard deviation (Figure 2g) is used to characterize the distribution of those changes over the studied interval (see section 2.2 in Text S2 and Figure S7 for details). Three patterns of variability (labeled 1, 2, and 3 in Figure 2g) are distinguished: high variance levels are recorded during the glacial inception (interval 1) and over the early MIS 5e maximum and Termination II (interval 3); an interval of reduced variability (interval 2) is found in between.

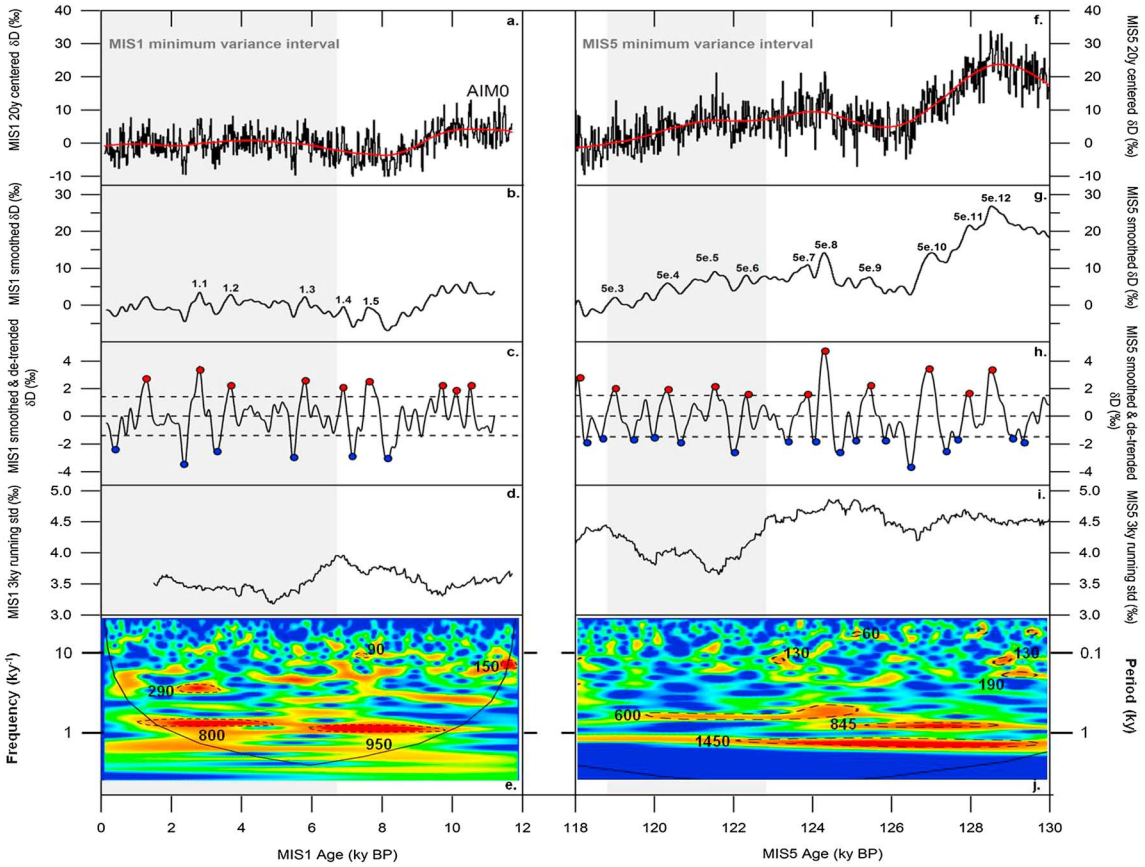

Figure 3. Comparison of (a–e) MIS 1 and (f–j) MIS 5e variance analysis over 12 kyr intervals. (a and f) Normalized 20 year resampled EDC δD records (black) and their associated multimillennial trend (red), calculated from a singular spectrum analysis method (SSA, see section 2.3 in Text S2). (b and g) Smoothed δD signals resulting from the 500 year binomial smoothing applied on the 20 year resampled data of Figures 3a and 3f. Detected events with respect to methodology displayed in Figures 3c and 3h are labeled for both MIS 1 and 5e intervals (in line with Figure 2e). (c and h) Detrended signals obtained by the subtraction of the red signals of Figures 3a and 3f from the black signals of Figures 3b and 3g. Black dashed lines represent the respective $\pm 1\sigma$ levels of the MIS 1 (1.4‰) and 5e (1.5‰) data distributions (Figure S5). Extreme isotopic values which do not range within the $\pm 1\sigma$ interval are highlighted by red (warm excursions) and blue points (cold excursions). Significant interglacial climatic subevents are commonly taken as sequences of two consecutive opposite excursions (see section 2.1 in Text S2 and Figure S5 for details). (d and i) Running standard deviation over 3 kyr of the black minus the red δD signals of Figures 3a and 3e (detrended signals). (e and j) Wavelet spectral analysis of the detrended signals. The spectral power is displayed in function of time (kyr B.P.), frequency (left axis, 1/kyr), and corresponding periodicity (right axis, kyr). Black contours delineate significant periodicities and black lines cones of influence (see section 2.3 in Text S2). Grey-shaded areas indicate minimum variance intervals, possibly reflecting true MIS 1 and 5e (interval 2) Antarctic "stable warm phases".

While intervals 1 and 3 show similar levels of variance, they are, however, expressed at different frequency ranges (Figure 2h, wavelet analysis method described in section 2.3 in Text S2). The variability within interval 1—exclusively expressed at centennial scale—clearly differs from the dominating millennial-scale variability identified during interval 3, which is also characterized by multidecadal to centennial significant periodicities. The minimum of variance recorded within interval 2 coincides with a loss of millennial variability and only one prevailing significant multicentennial periodicity (~600 years).

In Antarctica, the last interglacial period is characterized by three different climatic substages, composed of two transition phases surrounding a more stable climatic state. Our results emphasize a close link between those long-term trend changes and higher-frequency variability (additional statistical calculations in section 3.2 in Text S2). Interval 3—spanning Termination II and MIS 5e maximum—may thus be related to the climatic impact of the deglaciation history, driven by large insolation variations (Figure 2a). In the absence of information about volcanic and solar activity as well as about AMOC variability during MIS 5e, it is not possible to conclude about the causes of the detected millennial variability. Nevertheless, the two significant ~1100 year and ~1450 year periodicities identified over this period are similar to millennial periodicities commonly attributed to solar and AMOC imprints in MIS 1 climate proxy records [*Debret et al.*, 2009]. We also note that the maximum level of

variance occurs at the beginning of the EDC plateau following MIS 5e early optimum, coinciding with the sea level high stand due to reduced ice volumes in Greenland ice sheet [*Dutton and Lambeck*, 2012; *NEEM-community-members*, 2013] and strong presumptions of significant Antarctic ice volume loss [*Bradley et al*., 2012, 2013; *Holden et al*., 2010; *O'Leary et al*., 2013]. Increased freshwater fluxes from both hemispheres are known to potentially influence AMOC [*Galaasen et al*., 2014; *Oppo et al*., 2006; *Swingedouw et al*., 2009], with implications for Antarctic sea ice extent and climate [*Mathiot et al*., 2013].

The EDC δD plateau (122.8 kyr B.P.)—coinciding with local temperatures estimated ~2°C warmer than present day (Figure 2f) and a stabilized global sea level (Figure 2b)—is marked by a 20% decrease in variance occurring within 1.2 kyr. While the EDC δD values start to slowly decrease, the variance level gradually increases before reaching the same level as during interval 1. This 4 kyr long period (interval 2 between 122.8 ± 1.5 and 118.8 ± 1.5 kyr B.P.) characterized by a minimum of variability is here proposed to represent the MIS 5e Antarctic "stable warm phase." Similarly, a 20% decrease in variance (within 1.7 kyr) is detected at 6.7 kyr B.P. during MIS 1 (Figure 3d). This makes the current Antarctic stable warm phase already 2.7 kyr longer than its MIS 5e analog (Figures 3d and 3i, grey areas).

Interval 1 and its strong centennial variability come along with the glacial inception and the associated decreasing orbital forcing (Figure 2a). We note that the increase in high-frequency variability predates the Antarctic cooling trend (Figure 2g). This feature—also observed at the end of MIS 11 [*Pol et al*., 2011]—supports the existence of early warning signals for critical climate dynamics transitions [*Scheffer et al*., 2009]. The absence of such significant variance increase during the last millennia could then be interpreted as the lack of any precursor sign for an imminent natural glacial inception.

This comparison between MIS 1 and MIS 5e Antarctic isotopic variances further confirms that the East Antarctica plateau experienced significantly more variable climate conditions during MIS 5e than during the last millennia—even within the most stable phases. Evidence based on the number and amplitudes of multicentennial climatic subevents detected during these two interglacials are here reinforced by a MIS 5e standard deviation being systematically 20% higher than during MIS 1 (Figures 3d and 3i).

4. Conclusion

Using new high-resolution EDC δD data, we have demonstrated the existence of submillennial-scale variability during MIS 5e, expanding the documentation of high-frequency variability during past interglacial periods. We have evidenced and numbered multicentennial climatic subevents occurring in an interglacial climatic context, but competing with the smallest AIM events of the last glacial period in terms of amplitude. While it is consequently reasonable to expect an imprint of such interglacial Antarctic events at larger scale, such investigation hangs on the emergence of new and well-synchronized records at sufficient resolution to possibly enable an accurate one-to-one identification. Three distinct intervals have further been highlighted in the EDC record, including two transition phases surrounding a period of minimum variability from 122.8 ± 1.5 to 118.8 ± 1.5 kyr B.P. The level of variability during this period remains higher than during the last 6.7 millennia of the current Holocene, thus providing first observational evidence that a polar climate warmer than today may also be more variable. The mechanisms causing such enhanced variability remain to be understood, but may involve ocean-atmosphere interactions in response to a different orbital context, and likely reduced austral sea ice extent and Antarctic ice volume [*Bradley et al*., 2012, 2013; *Holden et al*., 2010; *O'Leary et al*., 2013]. As previously observed in a comparable study focusing on MIS 11 [*Pol et al*., 2011], we have also detected an increase of MIS 5e climate variability prior to the glacial inception. We notice that the EDC δD Holocene record does not show any equivalent feature, thus possibly suggesting that the current interglacial—prior to recent increasing anthropogenic radiative perturbation—was not near its natural end.

In a context of growing interest for the last interglacial period as target for model evaluation [*Holden et al*., 2010; *Lunt et al*., 2013; *Stone et al*., 2013], our data add to benchmark Antarctic information for climate and ice sheet models and highlight new features of interglacial climate variability under warmer-than-today climatic conditions, which may be of prime importance for future climate scenarios. We, however, stress the need for additional palaeoclimatic records at sufficient temporal resolutions to further investigate the links between orbital contexts, mean climatic conditions, and higher-frequency variability. Efforts in synchronizing age scales also appear essential in order to assess the global features of climate variability during interglacial periods.

Acknowledgments

The authors want to address special thanks to Eric Wolff for his useful comments and support and to members of the Past Interglacials (PIGS) working group of the Past Global Changes (PAGES) project for discussions. This work is a contribution to the European Project for Ice Coring in Antarctica (EPICA), a joint European Science Foundation/European Commission (EU) scientific program, funded by the EU and by national contributions from Belgium, Denmark, France, Germany, Italy, Netherlands, Norway, Sweden, Switzerland, and the U.K. The main logistic support was provided by IPEV and PNRA. LSCE analytical work has been funded by EPICA-MIS, ANR PICC, and Dome A, and by the European Union's Seventh Framework Programme (FP7/2007-2013) under grant agreement 243908, "Past4Future. Climate change—Learning from the past climate." The authors thank the two anonymous reviewers for their constructive comments, which helped to improve the manuscript. This is EPICA publication no. 297, Past4Future contribution no. 74, and LSCE publication no. 5314.

The Editor thanks two anonymous reviewers for their assistance in evaluating this paper.

References

Allen, J. R. M., and B. Huntley (2009), Last Interglacial palaeovegetation, palaeoenvironments and chronology: A new record from Lago Grande di Monticchio, southern Italy, *Quat. Sci. Rev.*, *28*(15–16), 1521–1538.

Bauch, H. A., and E. S. Kandiano (2007), Evidence for early warming and cooling in North Atlantic surface waters during the last interglacial, *Paleoceanography*, *22*, PA1201, doi:10.1029/2005PA001252.

Bigler, M., R. Röthlisberger, F. Lambert, E. W. Wolff, E. Castellano, R. Udisti, T. F. Stocker, and H. Fischer (2010), Atmospheric decadal variability from high-resolution Dome C ice core records of aerosol constituents beyond the Last Interglacial, *Quat. Sci. Rev.*, *29*(1–2), 324–337.

Bazin, L., et al. (2013), An optimized multi-proxy, multi-site Antarctic ice and gas orbital chronology (AICC2012): 120–800 ka, *Clim. Past*, *9*(4), 1715–1731.

Braconnot, P., S. P. Harrison, M. Kageyama, P. J. Bartlein, V. Masson-Delmotte, A. Abe-Ouchi, B. Otto-Bliesner, and Y. Zhao (2012), Evaluation of climate models using palaeoclimatic data, *Nature Clim. Change*, *2*(6), 417–424.

Bradley, S. L., M. Siddall, G. A. Milne, V. Masson-Delmotte, and E. Wolff (2012), Where might we find evidence of a Last Interglacial West Antarctic Ice Sheet collapse in Antarctic ice core records?, *Global Planet. Change*, *88–89*, 64–75.

Bradley, S. L., M. Siddall, G. A. Milne, V. Masson-Delmotte, and E. Wolff (2013), Combining ice core records and ice sheet models to explore the evolution of the East Antarctic Ice sheet during the Last Interglacial period, *Global Planet. Change*, *100*, 278–290.

Capron, E., et al. (2010), Millennial and sub-millennial scale climatic variations recorded in polar ice cores over the last glacial period, *Clim. Past*, *6*(3), 345–365.

Debret, M., D. Sebag, X. Crosta, N. Massei, J. R. Petit, E. Chapron, and V. Bout-Roumazeilles (2009), Evidence from wavelet analysis for a mid-Holocene transition in global climate forcing, *Quat. Sci. Rev.*, *28*(25–26), 2675–2688.

Deser, C., A. Phillips, V. Bourdette, and H. Teng (2012), Uncertainty in climate change projections: The role of internal variability, *Clim. Dyn.*, *38*(3–4), 527–546.

Drysdale, R. N., J. C. Hellstrom, G. Zanchetta, A. E. Fallick, M. F. Sánchez Goñi, I. Couchoud, J. McDonald, R. Maas, G. Lohmann, and I. Isola (2009), Evidence for obliquity forcing of glacial termination II, *Science*, *325*(5947), 1527–1531.

Dutton, A., and K. Lambeck (2012), Ice volume and sea level during the Last Interglacial, *Science*, *337*(6091), 216–219.

Ekaykin, A. A., V. Y. Lipenkov, N. I. Barkov, J. R. Petit, and V. Masson-Delmotte (2002), Spatial and temporal variability in isotope composition of recent snow in the vicinity of Vostok station, Antarctica: Implications for ice-core record interpretation, *Ann. Glaciol.*, *35*(1), 181–186.

EPICA-community-members (2004), Eight glacial cycles from an Antarctic ice core, *Nature*, *429*(6992), 623–628.

EPICA-community-members (2006), One-to-one coupling of glacial climate variability in Greenland and Antarctica, *Nature*, *444*(7116), 195–198.

Galaasen, E. V., U. S. Ninnemann, N. Irvalı, H. F. Kleiven, Y. Rosenthal, C. Kissel, and D. A. Hodell (2014), Rapid reductions in north Atlantic deep water during the peak of the last interglacial period, *Science*, *343*(6175), 1129–1132.

Govin, A., et al. (2012), Persistent influence of ice sheet melting on high northern latitude climate during the early Last Interglacial, *Clim. Past*, *8*(2), 483–507.

Holden, P. B., N. R. Edwards, E. W. Wolff, N. J. Lang, J. S. Singarayer, P. J. Valdes, and T. F. Stocker (2010), Interhemispheric coupling, the West Antarctic Ice Sheet and warm Antarctic interglacials, *Clim. Past*, *6*(4), 431–443.

Imbrie, J., J. Hays, D. Martinson, A. McIntyre, A. Mix, J. Morley, N. Pisias, W. Prell, and N. Shackleton (1984), The orbital theory of Pleistocene climate: Support from a revised chronology of the marine d18 O record, in *Milankovitch and Climate*, edited by A. Berger et al., pp. 269–305, D. Reidel, Hingham, Mass.

Jouzel, J., et al. (2007), Orbital and millennial Antarctic climate variability over the past 800,000 years, *Science*, *317*(5839), 793–796.

Kawamura, K., S. Aoki, T. Nakazawa, A. Abe-Ouchi, and F. Saito (2010), Timing and duration of the last five interglacial periods from an accurate age model of the Dome Fuji Antarctic ice core, Abstract#PP43D-04 presented at 2010 Fall Meeting, AGU.

Kopp, R. E., F. J. Simons, J. X. Mitrovica, A. C. Maloof, and M. Oppenheimer (2009), Probabilistic assessment of sea level during the last interglacial stage, *Nature*, *462*(7275), 863–867.

Koutsodendris, A., A. Brauer, H. Pälike, U. C. Miller, P. Dulski, A. F. Lotter, and J. Pross (2011), Sub-decadal- to decadal-scale climate cyclicity during the Holsteinian interglacial (MIS 11) evidenced in annually laminated sediments, *Clim. Past*, *7*(3), 987–999.

Lambert, F., B. Delmonte, J. R. Petit, M. Bigler, P. R. Kaufmann, M. A. Hutterli, T. F. Stocker, U. Ruth, J. P. Steffensen, and V. Maggi (2008), Dust-climate couplings over the past 800,000 years from the EPICA Dome C ice core, *Nature*, *452*(7187), 616–619.

Loulergue, L., F. Parrenin, T. Blunier, J. M. Barnola, R. Spahni, A. Schilt, G. Raisbeck, and J. Chappellaz (2007), New constraints on the gas age-ice age difference along the EPICA ice cores, 0–50 kyr, *Clim. Past*, *3*(3), 527–540.

Loulergue, L., A. Schilt, R. Spahni, V. Masson-Delmotte, T. Blunier, B. Lemieux, J.-M. Barnola, D. Raynaud, T. F. Stocker, and J. Chappellaz (2008), Orbital and millennial-scale features of atmospheric CH4 over the past 800,000 years, *Nature*, *453*(7193), 383–386.

Lunt, D. J., et al. (2013), A multi-model assessment of last interglacial temperatures, *Clim. Past*, *9*(2), 699–717.

Luthi, D., et al. (2008), High-resolution carbon dioxide concentration record 650,000–800,000 years before present, *Nature*, *453*(7193), 379–382.

Martrat, B., J. O. Grimalt, C. Lopez-Martinez, I. Cacho, F. J. Sierro, J. A. Flores, R. Zahn, M. Canals, J. H. Curtis, and D. A. Hodell (2004), Abrupt temperature changes in the western Mediterranean over the past 250,000 years, *Science*, *306*(5702), 1762–1765.

Masson, V., et al. (2000), Holocene climate variability in Antarctica based on 11 ice-core isotopic records, *Quat. Res.*, *54*(3), 348–358.

Masson-Delmotte, V., et al. (2010), Abrupt change of Antarctic moisture origin at the end of Termination II, *Proc. Natl. Acad. Sci. U.S.A.*, *107*(27), 12,091–12,094.

Masson-Delmotte, V., et al. (2011), A comparison of the present and last interglacial periods in six Antarctic ice cores, *Clim. Past*, *7*(2), 397–423.

Mathiot, P., H. Goosse, X. Crosta, B. Stenni, M. Braida, H. Renssen, C. J. Van Meerbeeck, V. Masson-Delmotte, A. Mairesse, and S. Dubinkina (2013), Using data assimilation to investigate the causes of Southern Hemisphere high latitude cooling from 10 to 8 ka BP, *Clim. Past*, *9*(2), 887–901.

Mayewski, P. A., et al. (2004), Holocene climate variability, *Quat. Res.*, *62*(3), 243–255.

Milner, A. M., U. C. Müller, K. H. Roucoux, R. E. L. Collier, J. Pross, S. Kalaitzidis, K. Christanis, and P. C. Tzedakis (2013), Environmental variability during the Last Interglacial: A new high-resolution pollen record from Tenaghi Philippon, Greece, *J. Quaternary Sci.*, *28*(2), 113–117.

Müller, U. C., S. Klotz, M. A. Geyh, J. Pross, and G. C. Bond (2005), Cyclic climate fluctuations during the last interglacial in central Europe, *Geology*, *33*(6), 449–452.

NEEM-community-members (2013), Eemian interglacial reconstructed from a Greenland folded ice core, *Nature*, *493*(7433), 489–494.

Neumann, T. A., and E. D. Waddington (2004), Effects of firn ventilation on isotopic exchange, *J. Glaciol.*, *50*(169), 183–194.

O'Leary, M. J., P. J. Hearty, W. G. Thompson, M. E. Raymo, J. X. Mitrovica, and J. M. Webster (2013), Ice sheet collapse following a prolonged period of stable sea level during the last interglacial, *Nat. Geosci.*, *6*(9), 796–800.

Oppo, D. W., J. F. McManus, and J. L. Cullen (2006), Evolution and demise of the Last Interglacial warmth in the subpolar North Atlantic, *Quat. Sci. Rev.*, *25*(23–24), 3268–3277.

Parrenin, F., et al. (2007), The EDC3 chronology for the EPICA Dome C ice core, *Clim. Past*, *3*(3), 485–497.
Pol, K., et al. (2011), Links between MIS 11 millennial to sub-millennial climate variability and long term trends as revealed by new high resolution EPICA Dome C deuterium data—A comparison with the Holocene, *Clim. Past*, *7*(2), 437–450.
Ramseier, R. O. (1967), Self-diffusion of tritium in natural and synthetic ice monocrystals, *J. Appl. Phys.*, *38*(6), 2553–2556.
Scheffer, M., J. Bascompte, W. A. Brock, V. Brovkin, S. R. Carpenter, V. Dakos, H. Held, E. H. van Nes, M. Rietkerk, and G. Sugihara (2009), Early-warning signals for critical transitions, *Nature*, *461*(7260), 53–59.
Siegenthaler, U., et al. (2005), Stable carbon cycle–climate relationship during the Late Pleistocene, *Science*, *310*(5752), 1313–1317.
Sime, L. C., E. W. Wolff, K. I. C. Oliver, and J. C. Tindall (2009), Evidence for warmer interglacials in East Antarctic ice cores, *Nature*, *462*(7271), 342–345.
Spahni, R., J. Schwander, J. Flückiger, B. Stauffer, J. Chappellaz, and D. Raynaud (2003), The attenuation of fast atmospheric CH4 variations recorded in polar ice cores, *Geophys. Res. Lett.*, *30*(11), 1571, doi:10.1029/2003GL017093.
Spahni, R., et al. (2005), Atmospheric methane and nitrous oxide of the Late Pleistocene from Antarctic ice cores, *Science*, *310*(5752), 1317–1321.
Sprovieri, R., E. Di Stefano, A. Incarbona, and D. W. Oppo (2006), Suborbital climate variability during Marine Isotopic Stage 5 in the central Mediterranean basin: evidence from calcareous plankton record, *Quat. Sci. Rev.*, *25*(17–18), 2332–2342.
Stenni, B., V. Masson-Delmotte, E. Selmo, H. Oerter, H. Meyer, R. Röthlisberger, J. Jouzel, O. Cattani, S. Falourd, and H. Fischer (2010), The deuterium excess records of EPICA Dome C and Dronning Maud Land ice cores (East Antarctica), *Quat. Sci. Rev.*, *29*(1), 146–159.
Stenni, B., et al. (2011), Expression of the bipolar see-saw in Antarctic climate records during the last deglaciation, *Nat. Geosci.*, *4*(1), 46–49.
Stone, E. J., D. J. Lunt, J. D. Annan, and J. C. Hargreaves (2013), Quantification of the Greenland ice sheet contribution to Last Interglacial sea-level rise, *Clim. Past*, *9*(2), 621–639.
Swingedouw, D., T. Fichefet, H. Goosse, and M. Loutre (2009), Impact of transient freshwater releases in the Southern Ocean on the AMOC and climate, *Clim. Dyn.*, *33*(2), 365–381.
Tzedakis, P. C., D. Raynaud, J. F. McManus, A. Berger, V. Brovkin, and T. Kiefer (2009), Interglacial diversity, *Nat. Geosci.*, *2*(11), 751–755.
Wanner, H., et al. (2008), Mid- to Late Holocene climate change: An overview, *Quat. Sci. Rev.*, *27*(19–20), 1791–1828.
Wanner, H., O. Solomina, M. Grosjean, S. P. Ritz, and M. Jetel (2011), Structure and origin of Holocene cold events, *Quat. Sci. Rev.*, *30*(21–22), 3109–3123.
Wolff, E. W., et al. (2010), Changes in environment over the last 800,000 years from chemical analysis of the EPICA Dome C ice core, *Quat. Sci. Rev.*, *29*(1–2), 285–295.